

Oxidation Kinetics of UO_2 Pellets in Defective Fuel Rods and Its Effect on Fission Gas Release

Yang Hyun Koo and Dong Seong Sohn
Korea Atomic Energy Research Institute

Young Ku Yoon
Korea Advanced Institute of Science and Technology
(Received November 22, 1993)

노내 손상 핵연료의 산화거동 및 핵연료 산화가 핵분열기체 방출에 미치는 효과

구양현 · 손동성
한국원자력연구소

윤용구
한국과학기술원
(1993. 11. 22 접수)

Abstract

One of the major phenomena occurring in defective fuel rods is the oxidation of UO_2 fuel pellets from UO_2 to UO_{2+x} by the oxygen produced from the dissociation of the steam in the pellet-to-clad gap, which leads to the enhancement of fission gas release. In this paper, the oxidation kinetics of defective fuel rods was analyzed on the basis of operating conditions of the reactor and defective fuel rod itself. Oxidation kinetics of the fuel pellet was determined under the assumption that the gap is filled with the saturated steam of 150 atm and an enhancement factor for fission gas release was introduced to take into account the effect of fuel oxidation on fission gas release. Comparison with experimental data shows that the enhancement factor predicts well the increased fission gas release due to the oxidation of UO_2 fuel pellets.

요 약

손상 핵연료에서 발생하는 주요한 현상중의 하나는 수증기의 분해로 갭에 존재하는 산소에 의해 UO_2 가 UO_{2+x} 로 산화되고, 이로 인해 결정립내에서의 핵분열기체 확산계수가 증가하여 결과적으로 핵분열기체의 방출이 증대하는 현상이다. 본 논문은 일반적인 원자로 운전 조건하에서 원자로 및 손상 핵연료의 운전조건을 고려하여 소결체의 산화거동을 모사하고 이를 바탕으로 소결체 산화가 핵분열기체의 방출 증대에 미치는 영향을 분석하였다. 소결체 산화거동은 갭에는 150 기압의 포화된 순수한 수증기만이 존재한다는 가정하에 분석하였고, 산화에 의한 핵분열기체의 방출 증대 효과를 정량적으로 분석하기 위

해 방출증대 인자를 도입하였다. 실험치와 비교한 결과 방출증대 인자는 소결체 산화에 의한 핵분열기체의 방출증대 효과를 잘 예측하였다.

1. Introduction

When defects exist in fuel cladding, the oxygen contained in the steam or in the mixture of steam and water can oxidize UO₂ fuel pellets. This is very important from the viewpoint of fission gas release because the increase in oxygen-to-uranium (O/U) ratio leads to direct enhancement of the diffusion coefficient of fission gas [1]. It is evident that fission gas release is enhanced by the presence of steam in the atmosphere in which UO₂ is heated. Hence fission gas release from defective fuel rods in a PWR under accident conditions would be greater than that anticipated from intact fuel rods whose environment does not contain steam [2].

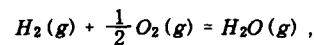
The enhanced release of fission gas from UO₂ fuel heated in steam as compared to that obtained in the inert or reducing atmosphere has been reported by many investigators. For example, Kurka et al. [3] found approximately 100-fold increase in the fractional fission gas release from defective fuel rods irradiated under conditions for which the UO₂ fuel was exposed to steam. They suggested that the increase is due to the oxidation of the UO₂ fuel. Schuster et al. [4] also reported that inferred effective diffusion coefficients for fission gases in defective fuel rods are about two orders of magnitude greater than those for intact ones. Therefore, the oxidation kinetics of the UO₂ fuel pellets must be analyzed to predict the fission gas release from the defective fuel rods.

The purpose of this paper is to investigate the oxidation kinetics of UO₂ pellets in defective fuel rods considering operating conditions of the reactor and defective fuel rod itself and the effect of UO₂ oxidation on the enhancement of fission gas release.

2. Oxidation Kinetics of UO₂ Pellets in Defective Fuel Rods

Fuel rod damage results in the exposure of the UO₂ fuel to steam at high temperature and high pressure. The chemical environment in the fuel-to-clad gap of defective fuel rod is complex due to oxidation of clad and UO₂ fuel and fission gas released from UO₂ fuel. Therefore, it is simply assumed in this paper that only pure steam exists in the gap and sufficient steam is supplied to the gap from the coolant through defect site. As can be seen in Fig. 1, when the steam is at typical reactor operating pressure (150 atm), the thermodynamic limit of fuel oxidation is greatly increased and O/U ratio can reach as high as 2.60 [5].

The oxygen potential of the gas phase that controls the oxidation of the UO₂ fuel is based on equilibrium of the reaction [6]:



for which the equilibrium constant can be expressed as

$$K = P_{H_2O} / P_{H_2} \sqrt{P_{O_2}} = \exp(-\Delta G^\circ / RT), \quad (1)$$

$$\text{where } \Delta G^\circ = -59.9 + 13.8 (T/10^3) \text{ Kcal/mol}, \quad (2)$$

and the partial pressures are expressed in atmospheres. For a pure steam environment under a total system pressure of P_T (atm), the oxygen potential of the gas mixture can be computed from

$$\bar{G}_{O_2} = RT \ln P_{O_2} = RT \ln (P_T X), \quad (3)$$

$$\text{where } X = P_{O_2} / P_T = (4 K^2 P_T)^{-1/3}.$$

The partial molar free energy can be expressed in terms of the partial molar entropy \bar{S}_{O_2} and enthalpy \bar{H}_{O_2} of oxygen as a function of deviation from stoichiometry x [7] (see Table 1):

Table 1. Thermodynamics of Oxygen in UO_{2+x} [7]

O/U Ratio	$\log P(\text{O}_2) = a + b/T$		$\bar{G}(\text{O}_2) = \bar{H}(\text{O}_2) - TS(\text{O}_2)$	
	a	-b	$-\bar{H}(\text{O}_2)$ cals/mole	$-\bar{S}(\text{O}_2)$ entropy units
2.0000	6.100	26,250	120,094	27.910
2.0010	4.563	22,848	104,528	20.877
2.0020	2.865	19,323	88,401	13.107
2.0030	1.800	17,195	78,667	8.233
2.0040	1.174	15,732	71,795	5.373
2.0050	0.664	14,684	67,179	3.037
2.0060	0.364	14,027	64,175	1.667
2.0070	0.391	13,788	63,080	1.790
2.0080	0.506	13,821	63,230	2.315
2.0090	0.526	13,656	62,476	2.406
2.0100	0.783	13,734	62,833	3.580
2.0110	0.629	13,517	61,841	2.877
2.0120	0.689	13,496	61,745	3.152
2.0130	0.775	13,509	61,807	3.547
2.0140	0.846	13,512	61,818	3.873
2.0150	1.035	13,619	62,307	4.734
2.0160	0.998	13,555	62,014	4.565
2.0170	1.097	13,613	62,280	5.018
2.0180	1.168	13,637	62,391	5.343
2.0190	1.230	13,652	62,456	5.627
2.0200	1.572	13,795	63,112	7.194
2.0250	1.397	13,606	62,249	6.392
2.0375	2.242	14,290	65,377	10.257
2.0500	2.800	14,702	67,267	12.812
2.0625	3.447	15,192	69,491	15.772
2.0750	3.892	15,494	70,885	17.808
2.0875	4.308	15,781	72,199	19.710
2.1000	5.046	16,544	75,687	23.087
2.1125	4.951	16,133	73,808	22.652
2.1250	5.375	16,422	75,129	24.592
2.1375	5.438	16,217	74,192	24.877
2.1500	5.806	16,417	75,107	26.563
2.1625	5.924	16,221	74,213	27.104
2.1750	5.720	15,600	71,370	26.171
2.1875	5.863	15,429	70,587	26.824
2.2000	6.609	16,159	73,916	30.238
2.2125	7.445	16,997	77,760	34.061
2.2250	8.222	17,720	81,071	37.616
2.2375	9.629	18,834	86,168	42.405

$$\bar{G}_{O_2}(x) = \bar{H}_{O_2}(x) - T \bar{S}_{O_2}(x) . \quad (4)$$

The equilibrium deviation from stoichiometry x_e in Eq.(5) is, therefore, given by the value of x , which minimizes the difference relation [19]

$$x_e = \min [\bar{G}_{O_2} - \bar{G}_{O_2}(x)] . \quad (5)$$

Based on recent studies which have suggested that the kinetics of UO_2 oxidation in steam are controlled by a probable reaction at the solid/gas interface and not by oxygen diffusion in the solid [21], Cox et al. [8] suggested that the oxidation kinetics of UO_2 can be expressed by the following rate equation :

$$\frac{dx}{dt} = -\alpha [x(t) - x_e] \left(\frac{S}{V} \right)_c , \quad (6)$$

where t = time (s)

α = surface exchange coefficient of oxygen (cm/s)

$$= 36.5 \exp(-23,500/T) \text{ (cm/s)}$$

T = temperature (K)

$(S/V)_c$ = ratio of surface area to the volume for the specimen (cm^{-1})

x = deviation from stoichiometry in UO_{2+x}
 $= \text{O/U} - 2.00$

x_e = equilibrium stoichiometry deviation as defined by the oxygen potential in the gas phase.

The solution of the above equation gives the O/U ratio analytically as a function of time (burnup), temperature, and $(S/V)_c$ as follows :

$$x(t) = x_e + [x(0) - x_e] \exp \left[-\alpha \left(\frac{S}{V} \right)_c t \right] . \quad (7)$$

The equilibrium composition of reaction products can be obtained using the well established thermodynamic properties of UO_2 and its higher oxides when the temperature and oxygen potential of the gaseous environment are known (see Table 1). The data in Table 1 [7], however, is only valid up to U_4O_9 ($x=0.25$). Thus, it has been conservatively assumed that U_3O_8 ($x \approx 0.6$) is reached at equilibrium if x and temperature is greater than 0.25 and 1120°C (see Fig.1), respectively.

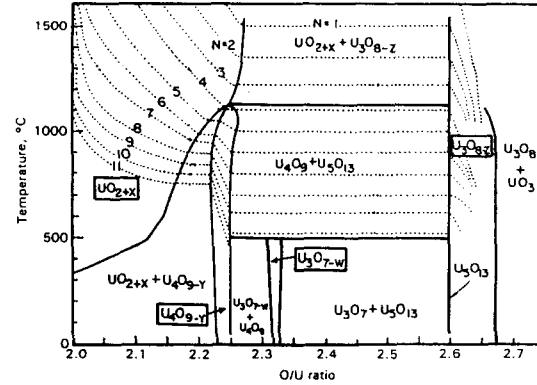


Fig. 1. The O/U Phase Diagram as A function of the O/U Ratio. The Dotted lines are Oxygen Pressure Isobars $\text{PO}_2=10^{-N}$ [6]

The oxygen/uranium phase diagram shown in Fig. 1 indicates that UO_2 can be oxidized to several higher oxides as a function of temperature. The UO_2 phase exists over a wide range of stoichiometry, and at temperatures above 1667°C , UO_{2+x} is the highest oxide which is stable as solid. Fig.1 also shows that phase stability is governed by the oxygen potential of the gas phase. Olander [6] has shown that the oxygen potential of steam is increased with pressure, and U_3O_8 could be formed in steam atmosphere if the pressure is sufficiently high.

Cox et al. [8] studied the kinetics of steam oxidation of UO_2 specimens (cylinders of 1.215 cm in diameter and 1.56 cm in height) at 1000, 1200, 1350, 1500 and 1650°C , respectively. Bittel et al. [9] also investigated the steam oxidation kinetics and oxygen diffusion in UO_2 at isothermal temperatures of 885 to 1835°C and at 1 atm. The samples whose diameter and height were 1.27 cm were sintered to 94 to 95% of theoretical density and a grain size of about $25 \mu\text{m}$.

The measured kinetics of the steam oxidation of UO_2 specimens obtained from these two experiments are compared with the predicted ones in Fig.2. Although slight deviation exists in the region of smaller O/U ratios, Eq.(7) yields results that are in

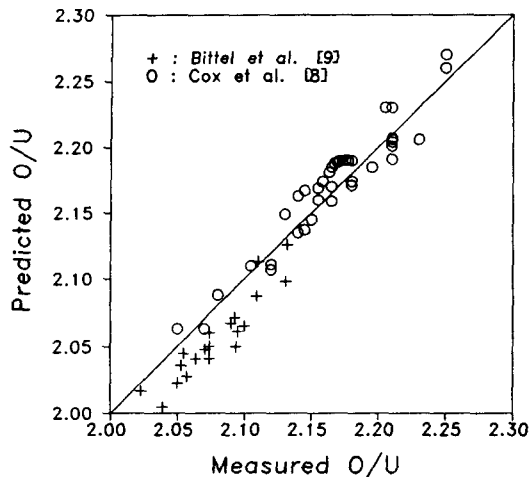


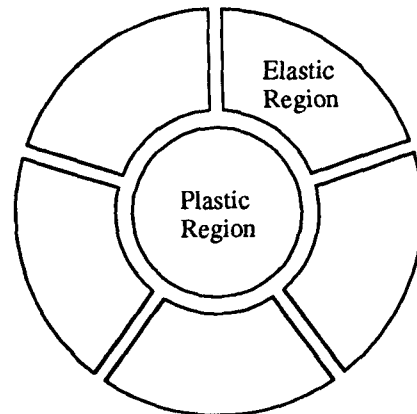
Fig. 2. Comparison of Measured Kinetics of Steam Oxidation of UO_2 and Predicted Ones.

good agreement with the data. Therefore, it can be concluded that the profile of O/U ratio across the fuel pellet contained in defective fuel rods can be obtained by using Eq.(7) if the steam pressure in the gap, the profiles of temperature and $(S/V)_c$ across the fuel pellet are known.

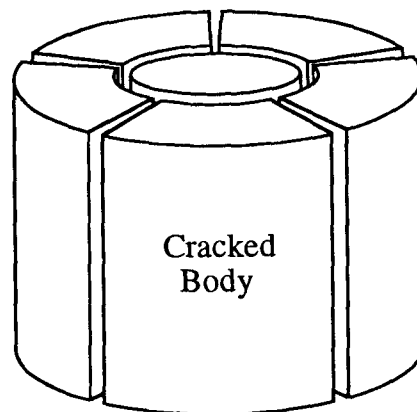
3. Analysis and Discussion

3.1. $(S/V)_c$ Profile across Fuel Pellet

According to the Notley's two zone model [10], UO_2 fuel pellet shows plasticity at temperatures above 1000°C when it is irradiated at least for 15 days. Therefore, it is assumed that the fuel pellet is composed of two regions depending on its temperature profile: (a) an inner plastic region whose temperature is higher than 1000°C and (b) an outer region whose temperature is lower than 1000°C and having a number of radial cracks through which gas release can occur (see Fig.3). Oguma [11] and Wood et al. [12] have shown that the number of pellet cracks increases almost linearly with linear heat generation rate and that the number of radial fuel cracks is about one-half of the linear heat generation



(a) Topview



(b) Overview

Fig. 3. Schematic Geometry of Cracked Fuel Pellet

rate (in kW/m). Once the linear heat generation rate and pellet dimensions are given, the ratio of surface area to volume for each cracked body $(S/V)_c$ can be obtained. Then using Eq.(7), O/U ratio profile across the fuel pellet can be calculated under the assumption that temperature and $(S/V)_c$ are constant during the entire time period. For the present analysis, the fuel pellet is divided into 10 equal volume annuli. Then $(S/V)_c$ for each annulus can be obtained on the basis of its average temperature. The average temperature for each annulus is calculated by the

CARO-D code [20] under typical operating conditions.

3.2. O/U Profile across Fuel Pellet

Fig.4 shows how the O/U ratio of a defective fuel rod changes as a function of temperature and time under the assumption that gap is filled with the saturated steam of 150 atm and $(S/V)c$ is 10 cm^{-1} . As might be expected, the higher the temperature is, the shorter the time required for reaching the equilibrium O/U ratio. This means that once the cladding failure occurs and the gap is filled with saturated steam, the central part of the pellet reaches the equilibrium O/U ratio in a relatively short time. On the other hand, the outer part takes longer time due to the slow oxidation kinetic behavior. This argument, of course, implies that there is an unlimited supply of steam to the UO_2 fuel pellet. In case that steam (i.e., oxygen) starvation occurs in the gap due to oxidation reaction of Zircaloy cladding, oxidation of UO_2 pellet would slow down because only a limited steam is available in the gap. Therefore, it must be noted that calculation results shown in Figs. 4 to 6 are thermodynamic limit that UO_2 can be oxidized.

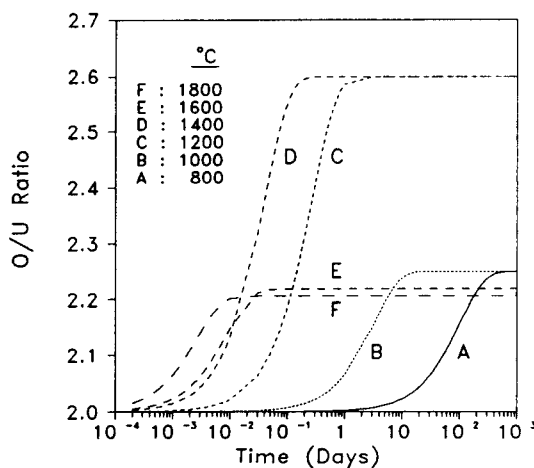


Fig. 4. O/U Ratio as a Function of Temperature and Time Elapsed After Fuel Rod Failure

For the pellet dimensions of the 17x17 KOFA (Korea Fuel Assembly) PWR fuel rod and for the linear heat generation rate of 200 W/cm, $(S/V)c$ for each annulus ranges from around 8 cm^{-1} to 15 cm^{-1} depending on its average temperature in case that the pellet is divided into 10 annuli of equal volume. Under these operating conditions, pellet centerline temperature does not exceed 1000°C during its most residence time and hence plastic region does not exist. In this respect, $(S/V)c$ is assumed to be 10 cm^{-1} for the following analyses. Fig.5 represents the O/U profile for a typical fuel rod as a function of operation time elapsed after the fuel rod failure when the linear heat generation rate is 200 W/cm and $(S/V)c$ for each annulus is taken to be 10 cm^{-1} . Under these operating conditions, as might be seen in Fig.4, the equilibrium O/U ratio is reached within about 40 days for the temperature higher than about 900°C . In a fuel rod with the linear heat generation rate of 200 W/cm, the pellet temperature, although this depends on the axial position and burnup, is generally above 900°C for the fractional pellet radius of less than about 0.4. Therefore, O/U

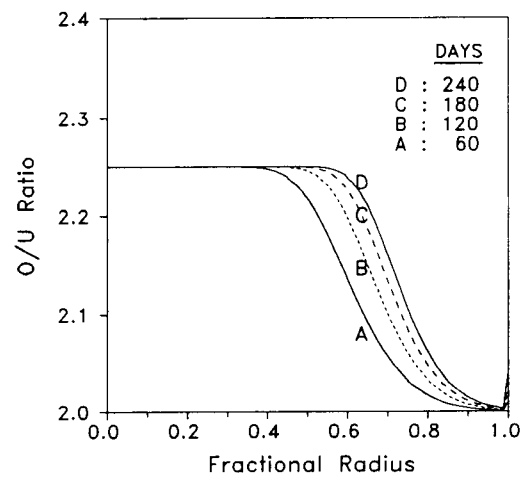


Fig. 5. O/U Profile in a Typical PWR Fuel Pellet as a Function of Time Elapsed After Fuel Rod Failure for the Linear Heat Generation Rate of 200 W/cm

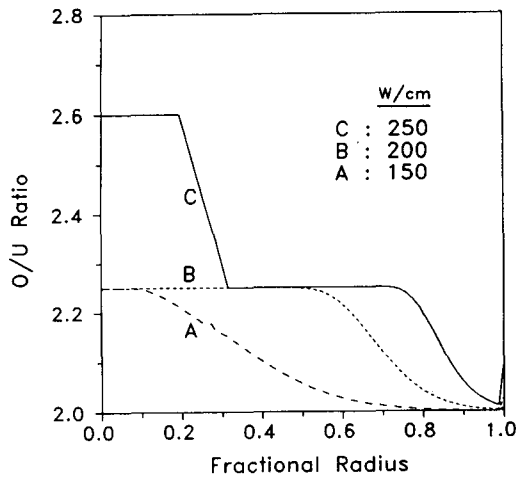


Fig. 6. O/U Profile for a Typical PWR Fuel Pellet as a Function of LHGR

ratio reaches its equilibrium value at a relatively short time in the inner part of the fuel pellet. However, at the outer region, O/U ratio continues to increase with time.

The O/U profile across a typical fuel pellet, which is predicted as a function of linear heat generation rate for the operation time of 150 days elapsed after fuel rod failure, is illustrated in Fig. 6. For 250 W/cm, O/U ratio can reach as high as 2.60 in the central part due to its temperature higher than 1120°C.

3.3. Diffusion Coefficient in Defective Fuel Rods

The diffusivity of fission gas in UO_{2+x} can be calculated as a function of temperature and deviation from stoichiometry x based on the analysis of Killen and Turnbull [13]. In this treatment, the diffusion coefficient is represented as a composite expression with components for intrinsic diffusion at high temperature, enhanced-vacancy production at intermediate temperature, and irradiation-enhanced (athermal) diffusion at low temperature :

$$D(x, T) = 7.6 \times 10^{-10} \exp(-7 \times 10^4/RT) + s^2 j_v (V' + V_u) + 2 \times 10^{-40} F \quad [\text{m}^2/\text{s}], \quad (8)$$

where

$$V' = -\frac{\alpha_s s^2}{2Z} \left\{ \left[1 + \frac{4KZ}{j_v \alpha_s s^2} \right]^{1/2} - 1 \right\}$$

= irradiation-induced vacancy concentration

V_u = uranium vacancy concentration

α_s = fixed sink strength ($\sim 10^{15} \text{ m}^{-2}$)

S = atomic jump distance ($\sim 3 \times 10^{-10} \text{ m}$)

Z = number of sites around a point at which recombination is inevitable (~ 100)

j_v = vacancy jump rate = $10^{13} \exp(-5.52 \times 10^{-4}/s \cdot \text{atom})$

K = defect production rate per atom ($\sim 2 \times 10^{-4}/s \cdot \text{atom}$)

F = fission rate (fissions/ $\text{m}^3 \text{ s}$).

According to Lidiard [14], the uranium vacancy concentration V_u as a function of the deviation from stoichiometry x is given by

$$V_u = (Sx^2/F_o^2) [0.5 + (F_o/x^2) + 0.5(1 + 4F_o/x^2)^{1/2}], \quad (9)$$

where

$$S = \exp(-147.2 \text{ kcal}/RT),$$

$$F_o = \exp(-71.3 \text{ kcal}/RT).$$

Since V_u is only a function of x , the diffusion coefficient of fission gas in defective fuel rods can be obtained once temperature and x are known. Fig. 7 shows that the diffusivity of fission gas is enhanced by a factor of about 1000 for U_4O_9 ($x=0.25$), whereas it only increases by an additional factor of 10 with oxidation to U_3O_8 ($x=0.66$) at a temperature of 1000°C ($10^4/T=7.8$). This means that gas release is not strongly sensitive to the formation of the higher oxide states. This result is consistent with fuel oxidation experiments where greater increase in release for Cs^{137} occurred at lower values of x [15].

3.4. Derivation of Enhancement Factor for Fission Products Release

The fractional release of fission gas during post-irradiation annealing experiment is given by [16]

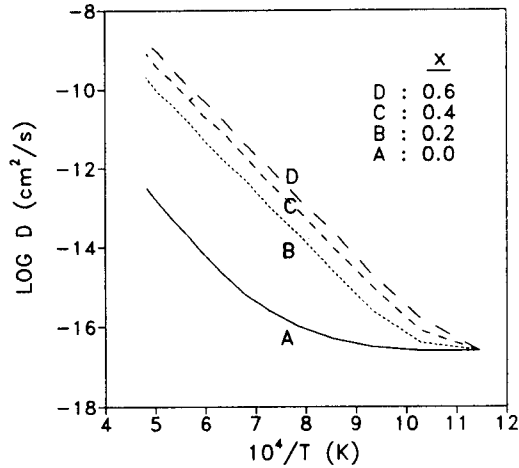


Fig. 7. In-Pile Diffusion Coefficient of Fission Gases as a Function of x (Deviation From Stoichiometry)

$$f = 6 \left(\frac{Dt}{\pi a^2} \right)^{1/2} - 3 \left(\frac{Dt}{\pi a^2} \right). \quad (10)$$

For most purposes the second term in Eq.(10) can be disregarded and the fractional release can be approximated as

$$f = 6 \left(\frac{Dt}{\pi a^2} \right)^{1/2}. \quad (11)$$

To confirm whether the effect of UO₂ oxidation on the enhancement of fission gas release can be described appropriately using the diffusion coefficient

given by Eq.(8), that is, fission gas release can be predicted as a function of deviation from stoichiometry x , the following two enhancement factors are introduced:

Measured enhancement factor $\equiv f(x)/f(0)$,

Predicted enhancement factor $\equiv \left(\frac{D(x,T)t}{D(0,T)t} \right)^{1/2}. \quad (12)$

Shiba [17] measured the release of iodine and xenon from UO₂ as a function of the O/U ratio with all the other parameters fixed. Table 2 gives the relevant data required for comparison between predicted and measured enhancement factors. Fig.8 shows that the total release of iodine increases monotonously with the O/U ratio except at the O/U ratio of 2.25 (U₄O₉). The enhancement factor for U₄O₉ is very low due to the fact that its stoichiometric structure exhibits higher stability than nonstoichiometric one [18]. The predicted enhancement factors for iodine shown in Fig.8 are based on the assumptions that the samples were irradiated only at 950°C and that iodine was released at this temperature only. These assumptions are reasonable because almost all the release occurred in the temperature range of 900 to 1000°C as was observed in Shiba's experiment [17]. Comparison between the predicted and measured enhancement factors shows good agreement for iodine, and this is the basis on which the prediction of fission gas release from UO_{2+x} can be made using the diffusion coefficient given in Eq.

Table 2. Comparison between Measured and Predicted Enhancement Factors for Fission Gas Release

O/U	x	$f(x)$	$f(x)/f(0)$	$D(x, T)t$	$[D(x, T)t/D(0, T)t]^{1/2}$
2.00	0.00	0.019	1.0	1.03E-13	1.0
2.04	0.04	0.078	4.2	5.65E-13	2.3
2.10	0.10	0.136	7.2	3.35E-12	5.7
2.14	0.14	0.162	8.6	6.55E-12	8.0
2.20	0.20	0.216	11.5	1.34E-11	11.4
2.33	0.33	0.219	11.7	3.63E-11	17.1
2.60	0.60	0.379	20.2	1.20E-10	28.4
2.62	0.62	0.433	23.0	1.28E-10	29.1

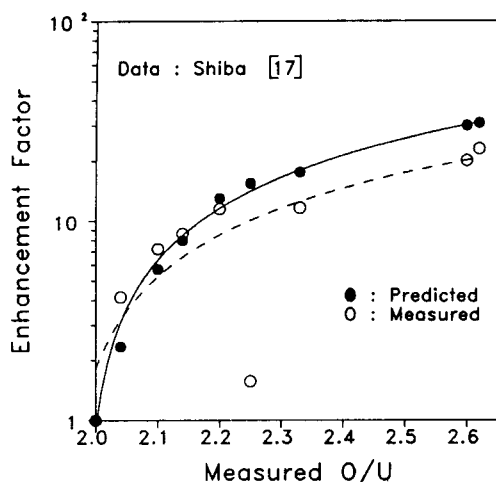


Fig. 8. Enhancement Factor for Fission Gas Release.

(8). Slight difference at higher O/U ratio seems to originate from the fact that while the effect of irradiation-enhanced vacancy concentration on the enhancement of fission gas release is considered in the present analysis, actual observation was made in the absence of this effect, that is, under post-irradiation annealing conditions.

4. Conclusions

The following conclusions can be drawn from this study:

1. The oxidation kinetics of defective fuel rod was analyzed on the basis of operating conditions of the reactor and defective fuel rod itself under the assumption that the gap is filled with saturated pure steam.
2. Based on the O/U ratio, an enhancement factor for fission gas release is introduced to take into account the effect of fuel oxidation on fission gas release. Comparison of predicted results with experimental data shows that the enhancement factor is useful for the prediction of increase in fission gas release due to fuel oxidation.

References

1. G.T. Lawrence, *J. Nucl. Mater.*, 71, 195 (1978).
2. D. Cubicciotti, *Nucl. Tech.*, 53, 5 (1981).
3. G. Kurka, A. Harrer and P. Chenebault, *Nucl. Tech.*, 46, 571 (1979).
4. E. Schuster et al., *Nucl. Eng. Des.*, 64, 81 (1981).
5. K. Naito and K. Kamegashira, *Adv. Nucl. Sci. Tech.*, 9, 99 (1976).
6. D.R. Olander, *Nucl. Tech.*, 74, 215 (1985).
7. P.O. Perron, "Thermodynamics of Non-Stoichiometric Uranium Dioxide," AECL-3072 (1968).
8. D.S. Cox, F.C. Iglesias et al., "Oxidation of UO_2 in Air and Steam with Relevance to Fission Product Release," Proc. Symp. on Chemical Phenomena Associated With Radioactivity during Severe Nuclear Plant Accidents, Anaheim, California, September, 1986, NUREG/CP-0078, pp. 2-35, U.S. NRC.
9. J.T. Bittel, L.H. Sjodahl, and J.F. White, *J. Am. Ceram. Soc.*, 52, 146 (1969).
10. M.J.F. Notley, *Nucl. Appl. Tech.*, 9, 195 (1970).
11. M. Oguma, *Nucl. Eng. Des.*, 76, 35 (1983).
12. J.C. Wood, B.A. Surette, I. Aitchison and W.R. Clendening, *J. Nucl. Mater.*, 88, 81 (1980).
13. J.C. Killen and J.A. Turnbull, "An Experimental and Theoretical Treatment of the Release of ^{85}Kr from Hyperstoichiometric Uranium Dioxide," Presented at Workshop on Chemical Reactivity of Oxide Fuel and Fission Product Release, Berkeley, U.K., April 7-9, 1987.
14. A.B. Lidiard, *J. Nucl. Mater.*, 19, 106 (1966).
15. C.E. Hunt, F.C. Iglesias and D.S. Cox, "Measured Release Kinetics of Iodine and Cesium from UO_2 at High Temperatures Under Reactor Accident Conditions," Proc. Int. Sem. Fission Product Transport Processes in Reactor Accidents, Dubrovnik, Yugoslavia, May, 1989.
16. D.R. Olander, *Fundamental Aspects of Nuclear Reactor Fuel Elements*, TID-26711-P1, p.301, Energy Research and Development Administration (1976).
17. K. Shiba, *J. Nucl. Mater.*, 57, 271 (1975).

18. R.M. Berman, M.L. Bleiberg, and W. Yeniscavich, *J. Nucl. Mater.*, 2, 129 (1960).
19. B.J. Lewis, F.C. Iglesias, D.S. Cox and E. Gheorghiu, *Nucl. Tech.*, 92, 353 (1990).
20. R. Eberle and I. Distler, "The KWU Fuel Rod Computer CARO," KWU Technical Report B111/E117/82 (1982).
21. J.A. Meachen, *Nucl. Energy*, 28, 4, 221 (1989).